# Liquidus in the $CO_2$ + and $N_2O$ + Hydrofluorocarbon Systems†

**Roman Stryjek,‡ Giovanni Di Nicola,*,§ and Fabio Polonara§**

Dipartimento di Energetica, Università Politecnica delle Marche, Ancona, Italy, and Institute of Physical Chemistry, Polish Academy of Sciences, Warsaw, Poland

The present paper summarizes and reinterprets the results for a series of measurements of solid−liquid equilibria for binary systems formed by carbon dioxide or nitrous oxide with a series of hydrofluorocarbons (fluoromethane, difluoromethane, trifluoromethane, pentafluoromethane, 1,1,1,2-tetrafluoroethane, 1,1,1-trifluoroethane, and 1,1-difluoroethane). All of the systems form eutectics. The contribution from heat capacity and activity coefficients to the liquidus courses represented by the Schröder equation were analyzed for each system included in the present study. The performed analysis showed that both mentioned contributions are small and, to a great extent, are mutually compensating each other and thus could be disregarded. The results showed that, for the systems under study, the liquidus curve down to the eutectic point may be represented by the Schröder equation involving two quantities only: the temperature at triple point and the enthalpy of fusion of the system components.

## Introduction

In industrial applications, the cascade refrigeration cycle is useful when low temperatures are required (i.e., below 233.15 K). The conventional cascade system often relies on R13 and R23 as refrigerants. Because of the heavy environmental impact of these two fluids, however, several natural refrigerants, that is, carbon dioxide and nitrous oxide, have recently been considered for use in cascade refrigeration systems. In particular, several studies evaluated ammonia as the high-stage fluid and carbon dioxide or nitrous oxide as the low-stage fluid. The lowest evaporator temperature achievable was limited by the melting temperature of carbon dioxide ($T_m$ = 216.58 K) and nitrous oxide ($T_m$ = 182.33 K). The lower temperatures needed in some applications can be achieved by using blends. As the second system's component, a series of the hydrofluorocarbons (HFCs) were chosen. The systematic study covered the experimental measurements of solid−liquid equilibria (SLE) of $CO_2$ and $N_2O$ + HFCs (R32, R125, R134a, R143a, R152a, R23, and R41)[1−7] by the Rossini method[8] and, finally, of *PVTx* by the isochoric method.[9−14] The *PVTx* data in the two-phase region enable VLE parameters to be derived using a flash method with the Carnahan−Starling−De Santis equation of state (CSD EOS).[15]

In this work, the SLE measurements were reinterpreted, also in the light of the vapor−liquid equilibria (VLE) assessments from the isochoric data. The SLE data are important as defining the lowest temperatures for the system applications in refrigeration.

## Experimental Data Discussion

The experimental isochoric and SLE data were obtained by experimental apparatuses presented elsewhere.[1−7,9−14] The information on the SLE data measurements along with the VLE data for corresponding binaries measured by the isochoric method is presented in Table 1. From the Table 1, it is easily evident that the temperatures of isochoric *PVTx* in two-phase region data are covering a higher temperature range than SLE data for which, obviously, the upper limit of temperature corresponds to the melting temperature of the solute or solvent, whatever is higher. Vice versa, the lower limit of the isochoric data corresponds either to the limit of the experimental feasibility of the setup or to the vapor pressures of the system under study. These two limitations result in a gap between the upper limit of temperature for the SLE data and the lower limit of temperature for the isochoric data. The consequences of that gap for the modeling of the SLE will be discussed more in detail below.

**Table 1. Temperature Ranges of SLE and Isochoric *PVTx* in Two-Phase Region Data**

| | SLE | | isochoric | | |
|---|---|---|---|---|---|
| system | *T*/K | ref | *T*/K | $K_{12}$ | ref |
| $CO_2$ + R32 | 132−217 | 2 | 254−293 | 0.0084 | 9 |
| $N_2O$ + R32 | 129−182 | 2 | 227−304 | 0.0317 | 12 |
| $CO_2$ + R23 | 118−217 | 6 | 253−283 | 0.0163 | 10 |
| $N_2O$ + R23 | 116−182 | 6 | 214−263 | 0.0139 | 12 |
| $CO_2$ + R125 | 158−217 | 1 | 253−304 | −0.0260 | 9 |
| $N_2O$ + R125 | 143−182 | 1 | 218−288 | −0.0270 | 13 |
| $CO_2$ + R41 | 125−217 | 7 | 217−288 | −0.0078 | 11 |
| $N_2O$ + R41 | 128−182 | 7 | 213−283 | 0.0126 | 12 |
| $CO_2$ + R152a | 146−217 | 3 | 223−288 | −0.0200 | 14 |
| $N_2O$ + R152a | 132−182 | 3 | | | |
| $CO_2$ + R134a | 156−217 | 4 | | | |
| $N_2O$ + R134a | 142−182 | 4 | | | |
| $CO_2$ + R143a | 156−217 | 5 | | | |
| $N_2O$ + R143a | 148−182 | 5 | | | |

The experimental SLE results showed that the presented $CO_2$ + and $N_2O$ HFCs binaries form the eutectic.[1−7] In the above-mentioned papers, the eutectic points (temperature and composition) were estimated from a graphical interpretation of the liquidus. The accuracy of the method depends on the shape of the liquidus curve and on the experimental data point distribution; hence, in this paper previous estimates are re-evaluated.

† Part of the "Workshop in Memory of Henry V. Kehiaian".

* Corresponding author. Tel.: +390712204277. Fax: +390712204770. E-mail: g.dinicola@univpm.it.
‡ Polish Academy of Sciences.
§ Università Politecnica delle Marche.

10.1021/je1007982 
Published on Web 10/12/2010

### Representation of the Liquidus by the Schröder Equation

The liquidus curve of eutectic systems is represented by the very well-known Schröder equation:[16]

$$\ln(x_2\gamma_2) = -\frac{\Delta H_m}{RT}\left(1 - \frac{T}{T_t}\right) + \frac{\Delta C_p}{R}\left(\frac{T_t - T}{T}\right) - \frac{\Delta C_p}{R}\ln\frac{T_t}{T} \quad (1)$$

where $\Delta H_m$ is the molar enthalpy of fusion, $T_t$ is the triple-point temperature, $\Delta C_p$ is the difference between the subcooled liquid solute and the solid solute, $\gamma$ is the activity coefficient, $x$ is the mole fraction, and the subscript 2 denotes the solute.

The use of eq 1 depends on the knowledge of the activity coefficient ($\gamma_2$) value; if $\gamma_2$ is unknown it seemed more suitable to use eq 1 in the following equivalent form:

$$\ln(x_2) = \frac{\Delta H_m}{RT_t} - \frac{\Delta H_m}{RT} + \frac{\Delta C_p}{R}\left(\frac{T_t - T}{T} - \ln\frac{T_t}{T}\right) - \ln(\gamma_2) \quad (2)$$

in which the liquidus curve is expressed as $\ln(x_2)$ values that come directly from the SLE experiment. An analysis, term after term of the Schröder equation, if expressed as in the form of eq 2 clearly shows the following:

- The first term takes a constant value dependent on the molar enthalpy of the solute fusion ($\Delta H_m$) at the triple-point temperature ($T_t$).

- The second term is again related to the $\Delta H_m$ value of solute, and it is linearly dependent on the inverse of temperature along the liquidus curve; so, these two terms, being dependent on the solute property, give a universal liquidus curve for each solute, independent of solvent down to the eutectic point, as far as the next terms are not contributing.

- The term dependent on the difference between the heat capacity of solute in subcooled liquid and solid state ($\Delta C_p$) has the same contribution for each solute to the liquidus curve, again being independent of the solvent, but it should be evident as a systematic deviation of the liquidus from the above-mentioned linear dependence. Going on a deeper analysis, its temperature dependence is given by the difference between the two terms $(T_t - T)/T$ and $\ln(T/T_t)$. Since these two terms have positive values not differing significantly over a quite wide temperature range, their contribution is canceled to a great extent. Keeping in mind that $(T_t - T)/T > \ln(T/T_t)$ always, the sign of the resulting value depends on the sign of the $\Delta C_p$ value.

By analyzing the SLE data of the $CO_2$ + HFCs and $N_2O$ + HFCs systems published successively by us,[1−7] we found that the liquidus representing $CO_2$ and $N_2O$ branches are well-represented by the Schröder equation in its simplified form:

$$\ln x_2 = -\frac{\Delta H_m}{RT}\left(1 - \frac{T}{T_t}\right) \quad (3)$$

after disregarding contributions from the $\Delta C_p$ and activity coefficient ($\gamma$) terms.

The observed regularities inspired us for a more detailed analysis of the possible contributions from these last two in the eq 2 terms. Unfortunately, because of the lack of the literature data on $C_p$ of subcooled liquids and VLE data on respective binaries at low temperatures, both of these terms had to be estimated. Additional simplification was based on assumptions that the solid solute is pure $CO_2$ or $N_2O$ and next that there is no solid solute phase transition below its triple point. The performed analysis of the course of the liquidus compositions shows some similarity to that performed by Preston and Prausnitz.[17] In our method we put an accent on the evaluation of possible contributions from $\Delta C_p$ and the evaluation of possible deviations from the Raoult's law based on VLE data analysis and their mutual coherence with SLE data. The contribution from $\Delta C_p$ values should be evident as systematic deviation from linearity is common from all systems with the same solutes, while the contribution from activity coefficient values should show an individual course of deviation for each binary system depending on the deviation from the Raoult's law. Thus, having previous observations in mind, the experimental SLE data were plotted as $\ln(x)$ with respect to $1/T$ in Figures 1 and 2, without any "a priori" assumption on possible $\Delta C_p$ and $\gamma$ contributions. In general, the Schröder equation represents experimental results for $CO_2$ and $N_2O$ as solutes with AAD (average absolute deviation) = 0.014 and AAD = 0.012, respectively. In addition, the distributions of deviations are clearly randomly distributed along temperature, as shown in Figures 3 and 4. A clearly greater deviation from the common

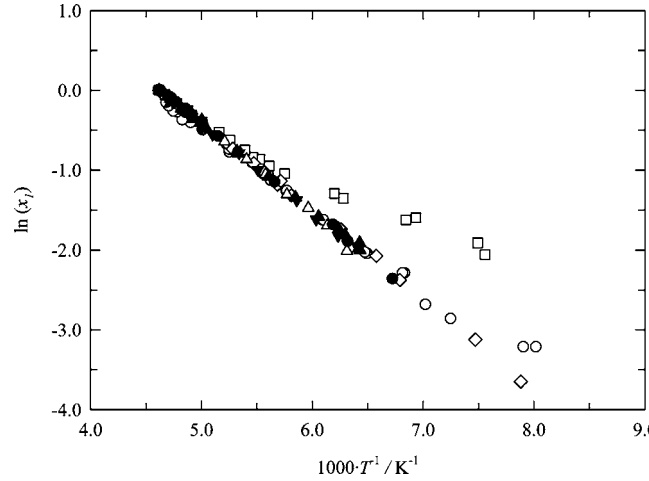


**Figure 1.** Experimental SLE data plotted as $\ln(x)$ versus $1000 \cdot T^{-1}$ for the $CO_2$ + HFCs binary systems. ○, $CO_2$ + R41; □, $CO_2$ + R32; ◇, $CO_2$ + R23; △, $CO_2$ + R125; ▲, $CO_2$ + R134a; ▼, $CO_2$ + R143a; ●, $CO_2$ + R152a.

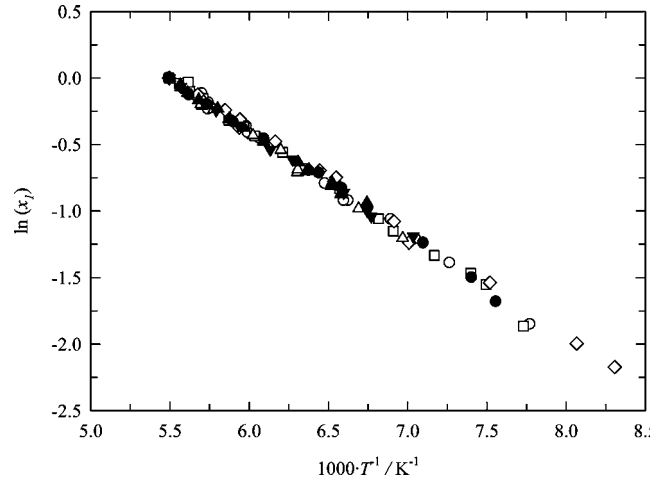


**Figure 2.** Experimental SLE data plotted as $\ln(x)$ versus $1000 \cdot T^{-1}$ for the $N_2O$ + HFCs binary systems. ○, $N_2O$ + R41; □, $N_2O$ + R32; ◇, $N_2O$ + R23; △, $N_2O$ + R125; ▼, $N_2O$ + R134a; ▲, $N_2O$ + R143a; ●, $N_2O$ + R152a.

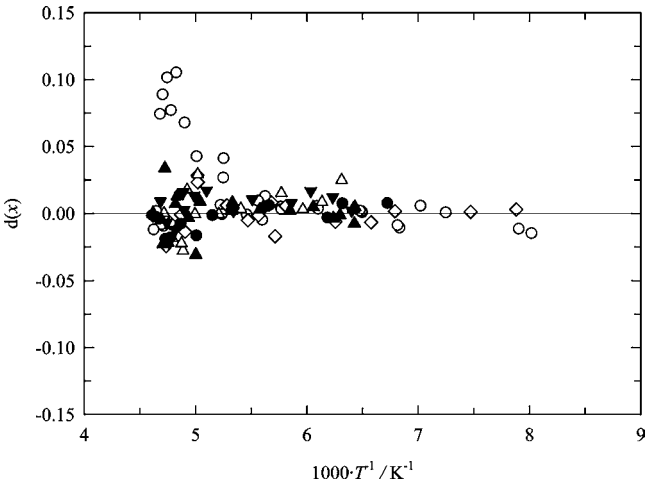


**Figure 3.** Deviations in composition, d($x$), for the $CO_2$ + HFCs binary systems, considering $CO_2$ as the solute. ○, $CO_2$ + R41; □, $CO_2$ + R32; ◇, $CO_2$ + R23; △, $CO_2$ + R125; ▼, $CO_2$ + R134a; ▲, $CO_2$ + R143a; ●, $CO_2$ + R152a.

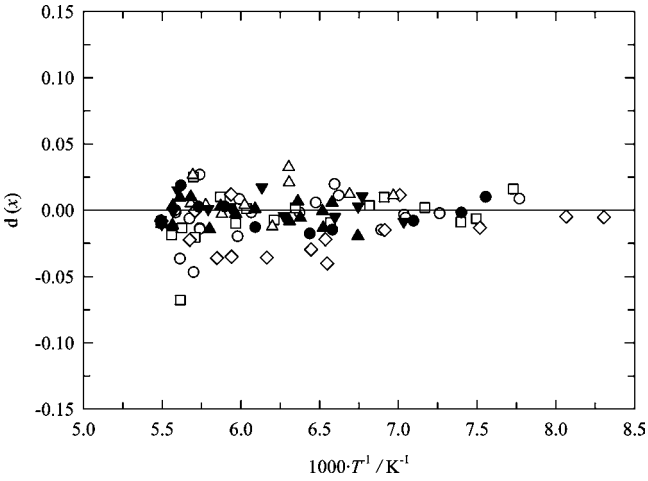


**Figure 4.** Deviations in composition, d($x$), for the $N_2O$ + HFCs binary systems, considering $N_2O$ as the solute. ○, $N_2O$ + R41; □, $N_2O$ + R32; ◇, $N_2O$ + R23; △, $N_2O$ + R125; ▼, $N_2O$ + R134a; ▲, $N_2O$ + R143a; ●, $N_2O$ + R152a.

linear trend is observed for the $CO_2$ + R32 system, only, which is not shown in the picture, being above scale. In addition, a greater deviation observed for some points of the $CO_2$ + R41 system, in our opinion, results from possible systematic greater experimental uncertainty in part of data collected during the cooling mode of experiment, as cannot be attributed to the applied model. It would be noted here that deviations were not observed for none of the $N_2O$ + HFCs systems.

***Analysis of the $\Delta C_p$ Contribution.*** To quantify the $\Delta C_p$ contribution, it is necessary to estimate both the $C_p(T)$ courses. Fortunately, $C_p$ for both solutes (i.e., $CO_2$ and $N_2O$) in the solid state is known.[18] The monotonous trend of $C_p$ does not suggest a marked contribution from the possible phase transition of solid solutes. $C_p$ of subcooled solutes were estimated from the literature data.[18,19] We decided to fix $\Delta C_p$ as a constant value, equal to the difference between liquid and solid heat capacities of $CO_2$ and $N_2O$ at the triple point. Finally, we adopted $\Delta C_p$ = 20.2 J·mol$^{-1}$·K$^{-1}$ and $\Delta C_p$ = 19.1 J·mol$^{-1}$·K$^{-1}$ for $CO_2$ and $N_2O$, respectively. Thus, we assumed that the subcooled liquid followed the same temperature trend than the solid solute.

The same methodology was applied if HFCs were considered as solutes. Regarding $\Delta C_p$ values, we could find only data for

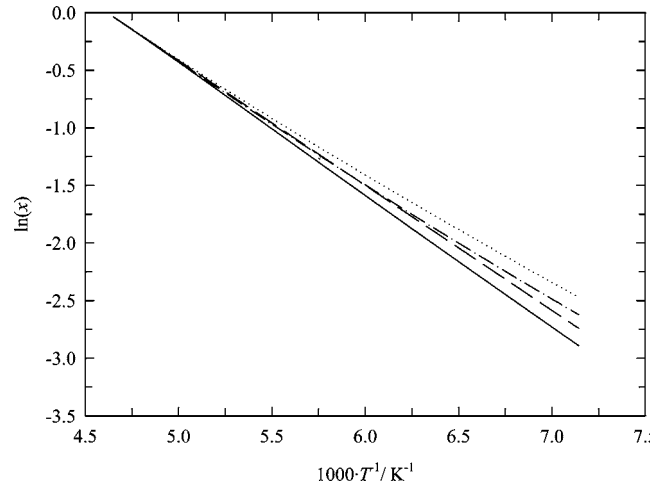


**Figure 5.** Behavior of the full (dashed−dotted line) and ideal (dashed line) Schröder equation, considering the $\Delta C_p$ (dotted line) and $\gamma$ contribution (solid line) for the $CO_2$ + HFCs binary systems.

R23 for which $C_p$ of the liquid and solid at triple point were 85.4 J·mol$^{-1}$·K$^{-1}$ and 70.5 J·mol$^{-1}$·K$^{-1}$, respectively, giving $\Delta C_p$ = 14.9 J·mol$^{-1}$·K$^{-1}$. This value is even smaller than the values above-reported for $CO_2$ and $N_2O$. For other HFCs, we could not find literature data enabling the estimation of $\Delta C_p$ because of the lack of information of $C_p$ of the solid state; thus, deviations for the liquidus of HFCs as solutes were calculated using the Schröder equation in the form of eq 3.

***Analysis of the Activity Coefficient Contribution.*** Our *PVTx* measurements by the isochoric methods for the respective $CO_2$ + HFCs and $N_2O$ + HFCs systems[9−14] at temperatures higher than SLE data showed that systems are showing small positive deviations in terms of Raoult's law; a very few additional VLE data from the literature for some $CO_2$ + HFCs,[20−29] measured at an even much higher temperature range than our data, showed a little bit greater but also positive deviations from Raoult's law. A comparable analysis of deviations from Raoult's law of all existing data for systems was considered (VLE and our isochoric) and showed that they have a slight trend of decreasing with the lowering of temperature. However, existing data could not be used for reliable extrapolation of VLE behavior at a much lower temperature range corresponding to our SLE data which would be needed to estimate realistic $\gamma$ values needed for the interpretation of the Schröder equation.

We performed some numerical analysis described below, if considering $CO_2$ and $N_2O$ as solutes. Thus, as a first assumption, we assumed few possible values of $g^E$ at the melting temperatures of the solutes varying from (25 to 100) J·mol$^{-1}$ at equal molar composition. For these values, the best $A$ = 200 J·mol$^{-1}$ value of two-suffix Margules equation used as temperature independent was found as being able to compensate $\Delta C_p$ contribution for both systems. The behavior is illustrated in Figures 5 and 6. The presented plots explain the experimentally observed good agreement of the course of solutes as represented by the simplified form of the Schröder equation, while contributions from $\Delta C_p$ term and $\gamma_2$ term may mutually compensate each other if system is showing small, positive deviation from the Raoult's law. Vice versa, for the same values of $\Delta C_p$ term and $\gamma_2$ term, the individual contribution of each term should be clearly evident in course of the liquidus. The presented plots confirmed a hypothesis that the systems presumably are showing a small positive deviation from the Raoult's law at temperatures corresponding to that of SLE measurements, even if accurate estimation of the behavior of VLE at that low temperatures by

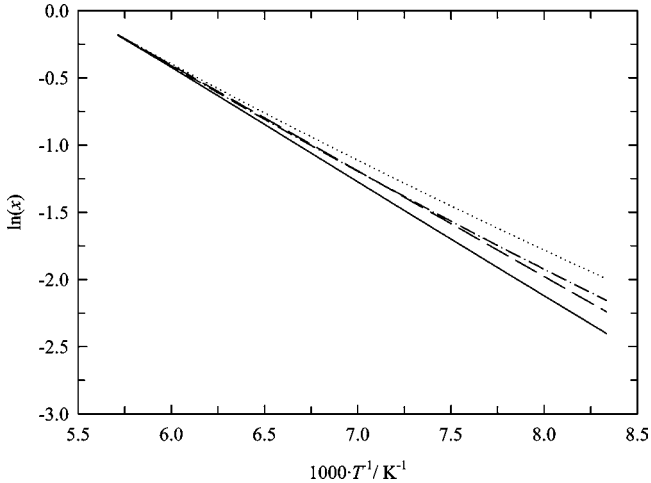


**Figure 6.** Behavior of the full (dash-dot line) and ideal (dashed line) Schröder equation, considering the $\Delta C_p$ (dotted line) and $\gamma$ contribution (solid line) for the $N_2O$ + HFCs binary systems.

**Table 2. Parameters for the Pure Fluids Involved in the Studied Binary Systems**

| compound | $T_f$ / K | $\Delta H_m$ / J·mol$^{-1}$ | $\Delta C_p$ / J·mol$^{-1}$·K$^{-1}$ |
|---|---|---|---|
| $CO_2$ | 216.59 | 9020 | 20.2 |
| $N_2O$ | 182.34 | 6540 | 19.1 |
| R23 | 118.02 | 4120 | 14.9 |
| R32 | 136.34 | 4356 | - |
| R41 | 129.82 | 4590 | - |
| R125 | 172.52 | 2249 | - |

the extrapolation of data measured at higher temperatures is obviously impossible. Considering the activity coefficients, their estimation should be coherent with estimated values of the molar excess Gibbs energy, $G^E(x)$, found using $\Phi-\Phi$ approach through the CSD EOS for the system considered. It means that the corresponding $A$ value of the two-suffix Margules equation, even if disregarding a small asymmetry in courses of $G^E(x)$, may be used to calculate the needed activity coefficient values at composition along the liquidus using the $\Delta H_m$ values reported in Table 2. The deviations in composition produced are shown in Figures 7 and 8.

Regarding HFCs as solutes, a possible $\Delta C_p$ contribution was discussed above. In the results of the actual state, the $\Delta C_p$ of

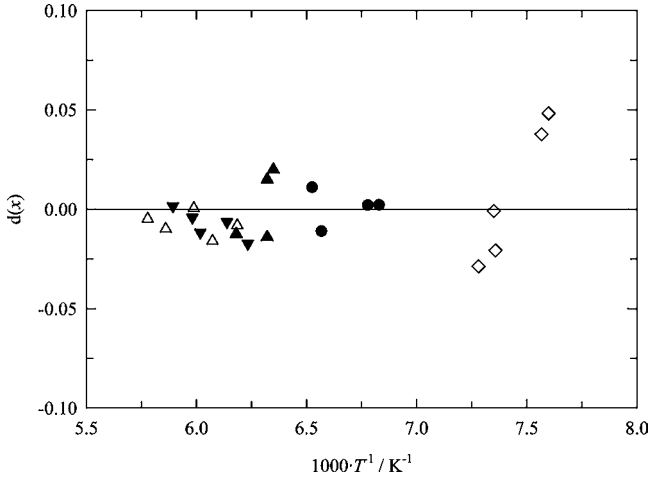


**Figure 7.** Deviations in composition, d($x$), for the $CO_2$ + HFCs binary systems, considering the HFCs as solutes. ◇, $CO_2$ + R23; △, $CO_2$ + R125; ▼, $CO_2$ + R134a; ▲, $CO_2$ + R143a; ●, $CO_2$ + R152a.

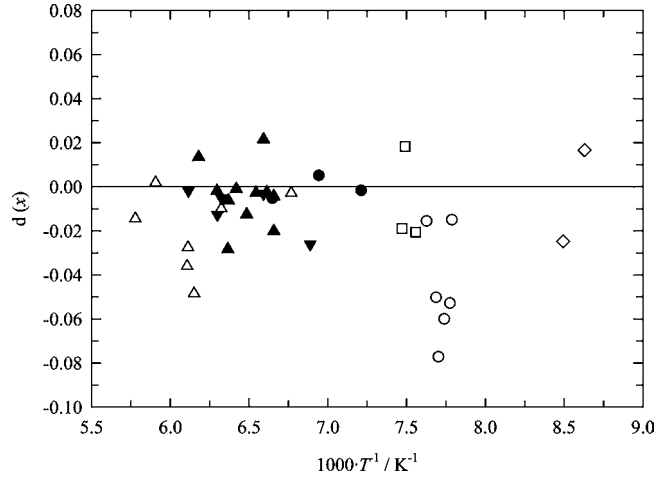


**Figure 8.** Deviations in composition, d($x$), for the $N_2O$ + HFCs binary systems, considering the HFCs as solutes. ○, $N_2O$ + R41; □, $N_2O$ + R32; ◇, $N_2O$ + R23; △, $N_2O$ + R125; ▼, $N_2O$ + R134a; ▲, $N_2O$ + R143a; ●, $N_2O$ + R152a.

**Table 3. VLE Parameters of the Literature Data**

| system | NP | $K_{12}$ | bias | AAD | $K_{12}(0)$ | $K_{12}(T)$ | bias | AAD | ref |
|---|---|---|---|---|---|---|---|---|---|
| $CO_2$ + R41 | 37 | −0.0059 | 0.12 | 0.73 | −0.0003 | 0.0002 | 0.02 | 0.33 | 20 |
| $CO_2$ + R32 | 55 | 0.0067 | 0.40 | 0.97 | 0.0127 | 0.0002 | 0.20 | 0.64 | 19 |
| $CO_2$ + R23 | 41 | 0.0131 | 0.16 | 0.73 | 0.0151 | 0.0003 | 0.10 | 0.38 | 21 |
| $CO_2$ + R125 | 22 | 0.0053 | 0.41 | 0.93 | −0.0401 | 0.0010 | 0.25 | 0.62 | 25 |
| $CO_2$ + R134a | 53 | −0.0069 | −0.26 | 1.37 | −0.0065 | −0.0001 | −0.10 | 1.35 | 22, 23 |
| $CO_2$ + R152a | 64 | 0.0044 | 0.45 | 1.36 | 0.0005 | 0.0003 | 0.12 | 0.68 | 26 |

HFCs as solutes has to be disregarded, and we believe that the term with the $\Delta C_p$ contribution is of negligible quantity due to the algebraic properties of its temperature dependence and small temperature range of that branch down to the eutectic point. Using eq 3, the AAD for HFCs as solutes was found to be AAD = 0.014 and AAD = 0.017 for the $CO_2$ + HFCs and $N_2O$ + HFCs systems, respectively. We find here that the overall deviations are very comparable with those found for $CO_2$ and $N_2O$ as solutes.

From the above-described analysis, it is evident that $\gamma$ has to be of the opposite sign and close to the $\Delta C_p$ contribution to follow the simplified form of the Schröder equation in which the terms dependent on $\Delta C_p$ and $\gamma$ are disregarded.

## On the Links between SLE and VLE Data

One of the problems in the SLE data interpretation using the Schröder equation is in the evaluation of the contribution of $\Delta C_p$ and $\gamma$ values in eqs 1 or 2. This aspect was analyzed more in detail, considering also that, for our binary systems and for our temperature ranges, there were no available literature data on the VLE. For higher temperatures, VLE data were measured for six binaries,[20−29] namely, $CO_2$ + R23, + R32, + R41, + R125, + R134a, and + R152a, but to our knowledge, none of the $N_2O$ + HFCs VLE data other than our sources was reported in the literature. Information on collated VLE data derived from our isochoric measurements, and in particular on the binary interaction parameters, $K_{12}$, are reported in Table 1, while information from the literature sources for the systems included in our SLE study are reported in Table 3, where the binary interaction parameters were presented both as fixed and as temperature-dependent values. Both the isochoric and the VLE data were correlated by the CSD EoS.[15] It is worth to point out that a satisfactory representation was obtained applying the CSD EoS with one adjustable parameter, excluding data near the

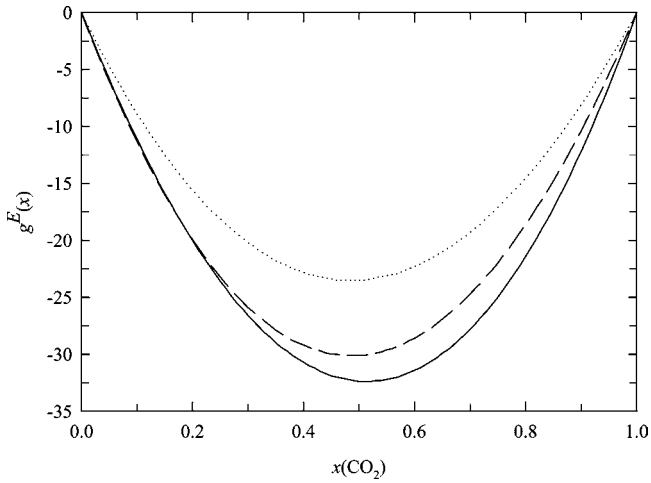


**Figure 9.** $G^E(x)$ values versus $CO_2$ composition for the R41 + $CO_2$ binary system at 240 K. Dotted line, $K_{12}$ as a constant value from ref 20; dashed line, $K_{12}$ as a temperature-dependent value from ref 20; solid line, $K_{12}$ from isochoric data.[11]

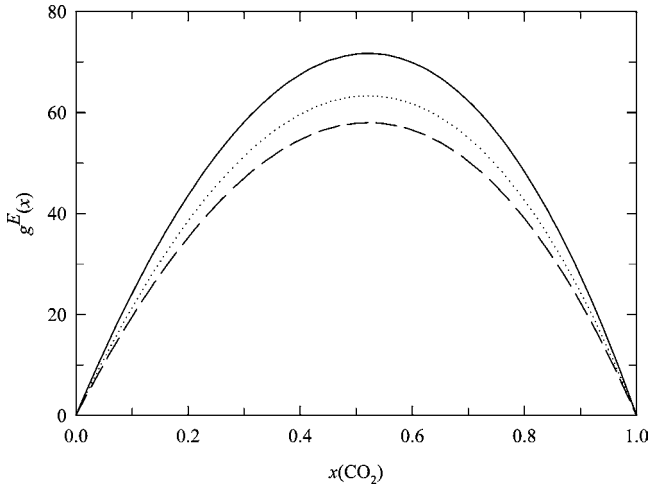


**Figure 10.** $G^E(x)$ values versus $CO_2$ composition for the R32 + $CO_2$ binary system at 240 K. Dotted line, $K_{12}$ as a constant value from ref 19; dashed line, $K_{12}$ as a temperature-dependent value from ref 19; solid line, $K_{12}$ from isochoric data.[9]

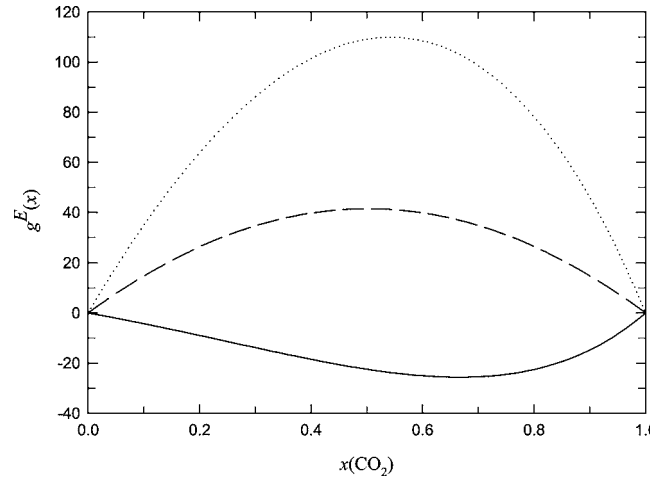


**Figure 11.** $G^E(x)$ values versus $CO_2$ composition for the R152a + $CO_2$ binary system at 240 K. Dotted line, $K_{12}$ as a constant value from ref 26; dashed line, $K_{12}$ as a temperature-dependent value from ref 26; solid line, $K_{12}$ from isochoric data.[14]

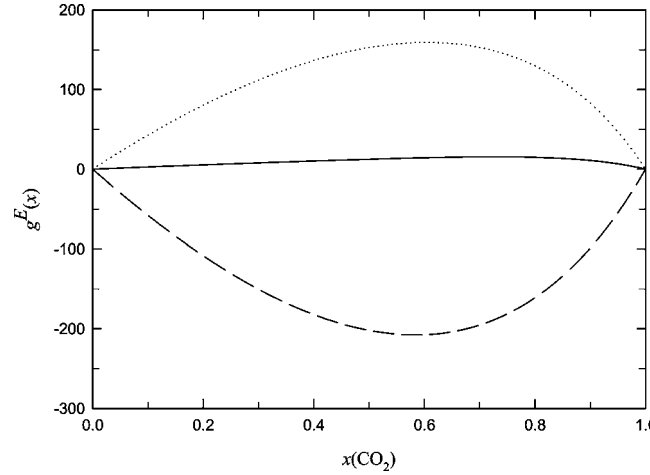


**Figure 12.** $G^E(x)$ values versus $CO_2$ composition for the R125 + $CO_2$ binary system at 240 K. Dotted line, $K_{12}$ as a constant value from ref 25; dashed line, $K_{12}$ as a temperature-dependent value from ref 25; solid line, $K_{12}$ from isochoric data.[9]

critical point.[28,29] Considering only the VLE data, the obtained results showed a slight improvement in terms of AAD and bias assuming the temperature dependence of $K_{12}$ as follows:

$$K_{12} = K_{12}(0)\cdot(T - 273.15)\cdot K_{12}(T) \qquad (4)$$

where the $K_{12}(0)$ and $K_{12}(T)$ parameters are reported in Table 3. In addition, for the $CO_2$ + R134a binary system, data were regressed, neglecting one source of data[24] that produced very high errors for one isotherm.

To get some information on the possible VLE behavior, the calculated $G^E$ are presented arbitrarily at $T = 240$ K for some $CO_2$ + HFCs systems, adopting $K_{12}$ values calculated both from isochoric and VLE literature data (the binary interaction parameters were considered both as constant and as temperature-dependent values) in Figures 9 to 12, respectively. For the R32 + $CO_2$ and R41 + $CO_2$ systems, a very good agreement between our isochoric and VLE data was found, while for R125 + $CO_2$ and R152a + $CO_2$, a small discrepancy was found. It is worth to note that small changes in VLE data representation may result in significant changes in $G^E$ courses, making it difficult to extrapolate the property to much lower temperatures. The graphs showed that $G^E$, even if not giving direct information on possible deviations from the Raoult's law for the considered systems, maybe can play some role also at much lower temperatures at which SLE was measured. So, as far as possible, considering fragmentary data, some analysis of possible liquid system behavior was carried out. Of course, considering the very complex intermolecular interaction between the HFCs, $CO_2$ and $N_2O$, it is impossible for us, decreasing the temperature by more than 100 K below the lowest limit of temperature for the present VLE data, to make a speculation about a possible trend in the VLE behavior.

***Derivation of the Eutectic Point.*** The composition of the eutectic for each binary system was found by solving two equations representing both liquidus branches. The $CO_2$-solute branch was represented by the average of the all-points representation (disregarding the $CO_2$ + R32 system); similarly, the $N_2O$-solute branch was represented by the averaging of all datum points for the respective systems. The HFC branches were represented by eq 3. The method adopted here is different from the method applied in our original papers, where the eutectic points were estimated system by system, so the results presented

**Table 4. Eutectic Point Estimated in Previous Papers[1−7] ($T_{old}$ and $x_{old}$) and in the Present Paper ($T_{new}$ and $x_{new}$)**

| system | $T_{old}$/K | $x_{old}$ | $T_{new}$/K | $x_{new}$ |
|---|---|---|---|---|
| $CO_2$ + R152a | 144 | 0.09 | 144.12 | 0.085 |
| $N_2O$ + R152a | 132 | 0.19 | 131.80 | 0.190 |
| $CO_2$ + R32 | 132 | 0.13 | 134.53 | 0.050 |
| $N_2O$ + R32 | 130 | 0.16 | 129.90 | 0.174 |
| $CO_2$ + R125 | 157 | 0.14 | 156.36 | 0.150 |
| $N_2O$ + R125 | 142 | 0.29 | 141.72 | 0.289 |
| $CO_2$ + R134a | 156 | 0.14 | 155.85 | 0.147 |
| $N_2O$ + R134a | 142 | 0.30 | 142.06 | 0.293 |
| $CO_2$ + R143a | 156 | 0.14 | 155.73 | 0.145 |
| $N_2O$ + R143a | 147 | 0.36 | 146.81 | 0.351 |

are slightly different. For the comparison, the old values along with those presently obtained are included in Table 4.

## Conclusion

The estimated contributions from the $\Delta C_p$ term are small; similarly, the evaluation of existing VLE and *PVTx* data for the $CO_2$ + and $N_2O$ + HFCs systems suggest that at low temperatures they show small but positive deviations from the Raoult's law, and the hence activity coefficient contribution may be of similar magnitude, thus resulting in compensation of these two contributions. The SLE results confirm our point, and it is clearly evident that the most simplified form of the Schröder equation is applicable to all of the systems studied, and small differences between calculated and experimental solid−liquid equilibrium data are acceptable as being not significantly greater than the estimated experimental uncertainty. Also, deviations in composition are clearly randomly distributed both if either plotted in respect to composition or temperature.

## Literature Cited


(1) Di Nicola, G.; Giuliani, G.; Polonara, F.; Stryjek, R. Solid−Liquid Equilibria for the $CO_2$ + R125 and $N_2O$ + R125 Systems: a New Apparatus. *J. Chem. Eng. Data* **2006**, *51*, 2209–2214.

(2) Di Nicola, G.; Giuliani, G.; Polonara, F.; Stryjek, R. Solid−Liquid Equilibria for the $CO_2$ + $N_2O$, $CO_2$ + R32 and $N_2O$ + R32 Systems. *Fluid Phase Equilib.* **2007**, *256*, 86–92.

(3) Di Nicola, G.; Giuliani, G.; Polonara, F.; Santori, G.; Stryjek, R. Solid−Liquid Equilibria for the $CO_2$ + R152a and $N_2O$ + R152a Systems. *J. Chem. Eng. Data* **2007**, *52*, 2451–2454.

(4) Di Nicola, G.; Santori, G.; Stryjek, R. Solid−Liquid Equilibria for the Carbon Dioxide + 1,1-Tetrafluoroethane and Nitrous Oxide + 1,1-Tetrafluoroethane Systems. *J. Chem. Eng. Data* **2008**, *53*, 1980–1983.

(5) Di Nicola, G.; Moglie, M.; Santori, G.; Stryjek, R. Solid−Liquid Equilibria for the $CO_2$ + R143a, and $N_2O$ + R143a Systems. *Int. J. Thermophys.* **2009**, *30*, 1155–1164.

(6) Di Nicola, G.; Giuliani, G.; Polonara, F.; Santori, G.; Stryjek, R. Solid−Liquid Equilibria for the $CO_2$ + R23, and $N_2O$ + R23 Systems. *Int. J. Thermophys.* **2010**; DOI 10.1007/s10765-008-0511-0.

(7) Di Nicola, G.; Moglie, M.; Polonara, F.; Santori, G.; Stryjek, R. Carbon Dioxide + Fluoromethane and Nitrous Oxide + Fluoromethane: Solid−Liquid Equilibria Measurements. *J. Chem. Eng. Data* **2010**; 10.1021/je100606z.

(8) Mair, B. J.; Glasgow, J. A. R.; Rossini, F. D. Determination of the freezing points and amounts of impurity in hydrocarbons from freezing and melting curves. *J. Res. Natl. Bur. Stand.* **1941**, *26*, 591–620.

(9) Di Nicola, G.; Pacetti, M.; Polonara, F.; Stryjek, R. Isochoric Measurements for $CO_2$ + R125 and $CO_2$ + R32 Binary Systems. *J. Chem. Eng. Data* **2002**, *47*, 1145–1153.

(10) Di Nicola, G.; Giuliani, G.; Polonara, F.; Stryjek, R. Isochoric Measurements of the R23 + $CO_2$ Binary System. *Fluid Phase Equilib.* **2003**, *210*, 33–43.

(11) Di Nicola, G.; Polonara, F.; Ricci, F.; Stryjek, R. *PVTx* Measurements for the R116 + $CO_2$ and R41 + $CO_2$ Systems. New Isochoric Apparatus. *J. Chem. Eng. Data* **2005**, *50*, 312–318.

(12) Di Nicola, G.; Giuliani, G.; Polonara, F.; Stryjek, R. *PVTx* Measurements for $N_2O$ + $CH_3F$, + $CH_2F_2$, and + $CHF_3$ Binary Systems. *Fluid Phase Equilib.* **2005**, *230*, 81–89.

(13) Di Nicola, G.; Giuliani, G.; Polonara, F.; Stryjek, R. Isochoric *PVTx* Measurements for the $N_2O$ + R125 Binary System. *J. Chem. Eng. Data* **2006**, *51*, 2041–2044.

(14) Di Nicola, G.; Polonara, F.; Santori, G.; Stryjek, R. Isochoric *PVTx* Measurements for the Carbon Dioxide + 1,1,Difluoroethane Binary System. *J. Chem. Eng. Data* **2007**, *52*, 1258–1261.

(15) De Santis, R.; Gironi, F.; Marrelli, L. Vapor−Liquid Equilibrium from a Hard-Sphere Equation of State. *Ind. Eng. Chem. Fundam.* **1976**, *15*, 183–189.

(16) Schröder, I. Über die Abhängigkeit der Löslichkeit eines festen Körpers von seiner Schmelztemperatur. *Z. Phys. Chem.* **1893**, *11*, 449–465.

(17) Preston, G. T.; Prausnitz, J. M. Thermodynamics of solid solubility in cryogenic solvents. *Ind. Eng. Process. Des. Dev.* **1970**, *9*, 264–271.

(18) *Selected Values of Hydrocarbons and Related Compounds*, Hydrocarbon Project; Thermodynamics Research Center, Texas A&M University: College Station, Texas, 1983.

(19) Ho, C. Y.; Liley, P. E.; Makita, T.; Tanaka, Y. Properties of Inorganic and Organic Fluids. *CINDAS Data Series on Material Properties*; Hemisphere: New York, 1988 p 1.

(20) Adams, R. A.; Stein, F. P. Vapor−Liquid Equilibria for Carbon Dioxide-Difluoromethane System. *J. Chem. Eng. Data* **1971**, *16*, 146–149.

(21) Outcalt, C. D.; Magee, J. W.; Scott, J. L.; Outcalt, S. L.; Haynes, W. M. *Selected Thermodynamic Properties for Mixtures of R-32 (Difluoromethane), R-134A (1,1,1,2-Tetrafluoroethane), R143A (1,1,1-Trifluoroethane), R-41 (Fluoromethane), R-290 (Propane), and R-744 (Carbon Dioxide)*; NIST Technical Note 1397; National Institute of Standards and Technology: Boulder, CO, 1997.

(22) Roth, M.; Lucas, K. Experimental vapor−liquid equilibria in the systems R22-R23, R22-$CO_2$, $CS_2$-R22, R23-$CO_2$, $CS_2$-R23 and their correlation by equations of state. *Fluid Phase Equilib.* **1992**, *73*, 147–166.

(23) Silva-Oliver, G.; Galicia-Luna, L. A. Vapor−liquid equilibria for carbon dioxide + 1,1,1,2-tetrafluoroethane (R-134a) systems at temperatures from 329 to 354 K and pressures up to 7.37 MPa. *Fluid Phase Equilib.* **2002**, *199*, 213–222.

(24) Duran-Valencia, C.; Pointurier, G.; Valtz, A.; Guilbot, P.; Richon, D. Vapor−Liquid Equilibrium (VLE) Data for the Carbon Dioxide ($CO_2$) + 1,1,1,2-Tetrafluoroethane (R134a) System at Temperatures from 252.95 to 292.95 K and Pressures up to 2 MPa. *J. Chem. Eng. Data* **2002**, *47*, 59–61.

(25) Lim, J. S.; Jin, J. M.; Yoo, K. P. VLE measurement for binary systems of $CO_2$ + 1,1,1,2-tetrafluoroethane (HFC-134a) at high pressures. *J. Supercrit. Fluids* **2008**, *44*, 279–283.

(26) Jeong, K.; Im, J.; Lee, S.; Kim, H. (Vapour + liquid) equilibria of the {carbon dioxide + pentafluoroethane (HFC-125)} system and the {carbon dioxide + dodecafluoro-2-methylpentan-3-one (NOVEC1230)} system. *J. Chem. Thermodyn.* **2007**, *39*, 531–535.

(27) Madani, H.; Valtz, A.; Coquelet, C.; Meniai, A. H.; Richon, D. (Vapor + liquid) equilibrium data for (carbon dioxide + 1,1-difluoroethane) system at temperatures from (258 to 343) K and pressures up to about 8 MPa. *J. Chem. Thermodyn.* **2008**, *40*, 1490–1494.

(28) Diefenbacher, A.; Crone, M.; Türk, M. Critical properties of $CO_2$, $CHF_3$, $SF_6$, ($CO_2$ + $CHF_3$), and ($CHF_3$ + $SF_6$). *J. Chem. Thermodyn.* **1998**, *30*, 481–496.

(29) Suehiro, Y.; Nakajima, M.; Yamada, K.; Uematsu, M. Critical parameters of $\{xCO_2 + (1-x)CHF_3\}$ for $x = (1.0000, 0.7496, 0.5013$ and $0.2522)$. *J. Chem. Thermodyn.* **1996**, *28*, 1153–1164.


Received for review August 2, 2010. Accepted October 3, 2010.

JE1007982